Ab initio estimate of temperature dependence of electrical conductivity in a model amorphous material: hydrogenated amorphous silicon

T. A. Abtew,* Mingliang Zhang,† and D. A. Drabold‡
Department of Physics and Astronomy, Ohio University, Athens, OH 45701
(Dated: February 1, 2008)

We present an *ab initio* calculation of the DC conductivity of amorphous silicon and hydrogenated amorphous silicon. The Kubo-Greenwood formula is used to obtain the DC conductivity, by thermal averaging over extended dynamical simulation. Its application to disordered solids is discussed. The conductivity is computed for a wide range of temperatures and doping is explored in a naive way by shifting the Fermi level. We observed the Meyer-Neldel rule for the electrical conductivity with E_{MNR}=0.06 eV and a temperature coefficient of resistance close to experiment for *a-Si:H*. In general, experimental trends are reproduced by these calculations, and this suggests the possible utility of the approach for modeling carrier transport in other disordered systems.

PACS numbers: 72.80.Ng, 72.20.-i,71.23.Cq

I. INTRODUCTION

Amorphous semiconductors are among the most important electronic materials. *a-Si:H* is the universal choice for TFT applications in laptop displays and important photovoltaic material. Thin films of a-Si:H are one of the promising active elements for uncooled microbolometers[1] as employed in focal plane arrays for night vision applications. Here, the temperature (T) dependence of the electrical conductivity, and the Temperature Coefficient of Resistance (TCR) is of paramount importance. Experiments suggest that there are well-defined conductivity regimes: variable-range hopping at the lowest temperatures, phonon-induced delocalization at higher temperatures and ultimately a metallic form of conduction (albeit with strong scattering). The venerable Meyer-Neldel rule[2,3] (MNR) correlating the exponential prefactor of the DC conductivity with the activation energy has been observed to be almost universally valid in disordered systems. A microscopic understanding of these effects is highly incomplete, though significant progress has been made on MNR[3,4].

Disordered solids pose definite challenges for transport modeling. The Boltzmann equation is best suited to long mean free paths, and is difficult to apply in these systems with localized states and defects. Moreover, the topological disorder must have a significant influence on the conduction and a realistic calculation of transport must include this disorder explicitly (eg through a credible structural model).

Modern density functional simulations of materials routinely provide the Kohn-Sham[5] eigenvalues and orbitals at each step in a thermal Molecular Dynamics (MD) simulation. The natural approximate connection of these quantities to electrical transport is provided by the Kubo-Greenwood formula (KGF)[6,7]. The first application of the KGF to an atomistic model with computed electronic structure was by Allen and Broughton[8] for (metallic) liquid Si with a tight-binding Hamiltonian. In this paper, we explore the utility of the KGF with Kohn-Sham spectral properties to estimate the temperature dependence of the conductivity in *a-Si* and *a-Si:H*. An adiabatic approximation is used for modeling the inelastic scattering of the phonons (by thermally averaging the KGF over a constant T MD trajectory). The underlying idea is that if the thermal fluctuations drive the unoccupied and occupied states close together (in the spirit of Landau-Zener[9] tunneling), then the energy conserving δ functions are nonzero, and a finite contribution to the conductivity is made by such instantaneous "snapshots" if the dipole matrix element is non-zero. Doping, the MNR and TCR are obtained and shown to be in reasonable agreement with measurements in *a-Si:H*. The results are sufficiently encouraging to justify a fuller exploration of the applicability of the method to disordered systems more generally, including other amorphous semiconductors and glasses and conducting polymers.

The paper is organized as follows. In Section II, we discuss the underlying logic of the approach and some salient previous calculations, In Section III, we briefly describe models and simulation procedures employed. In Section IV, we present results for *a-Si* and *a-Si:H* including the T-dependent conductivity, the effect of doping on the conductivity and a discussion of MNR and TCR for *a-Si:H*. Finally in Section V we draw conclusions.

II. APPROACH

A. Overview

Previous work on amorphous semiconductors and glasses has shown that Kohn-Sham eigenvalues conjugate to localized Kohn-Sham states are specially susceptible to the motion of the lattice[10,11] (thermal fluctuation in the atomic coordinates involved in localized states leads to a strong modulation of such eigenvalues and eigenvectors). Indeed, the RMS fluctuation of eigenvalues conjugate to localized eigenvectors is proportional to the localization of the eigenvector as measured by inverse participation ratio[11]. Localized states appear in the gap, or in the spectral band tails. Since they are

close to the Fermi level, they play a role in transport. The most elementary link between these states and energies and the conductivity is the KGF, which is a natural approach to strong scattering systems with short mean free paths. With this in mind, we use the Kubo formalism and current *ab initio* methods in conjunction with fairly realistic (structurally plausible) supercell models of *a-Si:H* to probe the temperature dependence of the DC conductivity. The novelty of our work lies in 1) using Kohn-Sham states and energies in Kubo's expression for the conductivity and 2) adopting a Born-Oppenheimer[12] like approximation of thermally averaging the KGF (using instantaneous atomic configurations obtained in the course of a thermal simulation at constant temperature as "snapshots"). Such an approach certainly has limitations: for low temperatures in which one expects variable range hopping between defects the correct link to first principle simulation would seem to require solutions of the time-dependent Kohn-Sham equations[14,15] or an approach more akin to a Miller-Abrahams[13] model of the conductivity. There are several studies which use the KGF to compute the static lattice conductivity of amorphous materials[16,17,18]. The computed conductivity vanishes for localized states in a static lattice.

As an alternative to the weak scattering theory of Ziman[19] for liquid metals, investigators have used the KGF with variants of Car-Parrinello[5] simulation to explore the conductivity of liquid metals including for example, l-NaSn alloys[20] and l-Na[21], with quite satisfactory results. It was found that Brillouin zone sampling had to be treated with care, which is reasonable for a metallic system. The success of such calculations is one motivation to extend the approach to doped amorphous semiconductors[22]. Another significant development of recent years is the Keldysh Green's function approach offered to properly handle the effects of contacts and finite potential drops for molecular electronics. An example of this approach is the code TRANSIESTA[23].

B. Connection to many-body formulation

The KGF has been applied on many occasions, and in liquids in a mode very similar to what we report here. However, there is usually no discussion of the underlying assumptions that connect the original many-body formulation of the KGF to its usual use with MD averages and single particle states. For example, the KGF as used in these computations is *not* formulated for use with inelastic processes, and thus the use of MD trajectories and averaging requires some discussion, which we offer in this section.

Consider a periodic perturbation H_{int}

$$H_{int} = Fe^{-i\omega t} + F^* e^{i\omega t} \tag{1}$$

acting on a system described via a many-body (electron and phonon) Hamiltonian H. The transition probability from initial state Ψ_i to final state Ψ_f in the interval $d\nu_f$ under the action of an external field (H_{int}) is[24]

$$\frac{2\pi}{\hbar}|\langle\Psi_f|F|\Psi_i\rangle|^2\delta(E_f - E_i - \hbar\omega)d\nu_f \tag{2}$$

where Ψ_f, Ψ_i are eigenstates of many-body Hamiltonian H

$$H\Psi_f = E_f\Psi_f, \quad H = H_0 + H^{e-ph}. \tag{3}$$

Here, E_f and Ψ_f may be estimated by the ordinary time-independent perturbation theory from the eigenfunctions $\Psi_p^{(0)}$ and eigenvalues $E_p^{(0)}$ of

$$H_0 = H_e + H_{ion}. \tag{4}$$

We adopt a Born-Oppenheimer description

$$H_0\Psi_p^{(0)} = E_p^{(0)}\Psi_p^{(0)} \tag{5}$$

with,

$$\Psi_p^{(0)} = \Phi_{e_p}\Theta_{v_p} \tag{6}$$

and Φ_{e_p} is a many electron wave function, Θ_{v_p} is a many phonon wave function. The perturbation solution of (3) is

$$\Psi_i = \sum_q a_{iq}\Psi_q^{(0)}, \quad a_{iq} = \delta_{iq} + a_{iq}^{(1)} + a_{iq}^{(2)} + \cdots \tag{7}$$

$$E_i = E_i^{(0)} + E_i^{(1)} + E_i^{(2)} + \cdots \tag{8}$$

Detailed expressions can be found in standard textbooks. The coupling H^{e-ph} between electrons and phonons need not be small, in principle eigenfunctions and eigenvalues of H can be calculated to any order of H^{e-ph}.

In $\omega \to 0$ limit, we only keep the interaction F_e between electrons and external field. Eq. 2 is modified to:

$$\begin{aligned}&\frac{2\pi}{\hbar}|\sum_{e_pe_q}[\sum_{v_p} a^*_{e_fv_f;e_pv_p}a_{e_iv_i;e_qv_p}]\langle\Phi_{e_p}|F_e|\Phi_{e_q}\rangle|^2\\ \times\ &\delta[(E_f^{(0)} + E_f^{(1)} + E_f^{(2)} + \cdots)\\ &-(E_i^{(0)} + E_i^{(1)} + E_i^{(1)} + \cdots) - \hbar\omega]d\nu_f\end{aligned} \tag{9}$$

Eq. 9 shows that for $\omega = 0$, the conservation of energy is for the whole (electron+phonon) system. Phonons may assist the transition between two many-electron states with different energy if the phonons can serve as source or sink of energy.

At finite temperature, initial state Ψ_i can be any one of all possible states. To calculate the total absorption power in a sample, we average initial state Ψ_i with Boltzmann weighting, and sum over all possible final states.

The Born-Oppenheimer approximation (BOA) starts with a stable lattice $A_0 : (X_1^0, Y_1^0, Z_1^0, \cdots X_N^0, Y_N^0, Z_N^0)$ as its zero order configuration. The sum over all possible phonon states v_p, one phonon, two-phonon, $\cdots$etc., in

Eq. 9 means that we explore all possible configurations of the lattice around our original conformation A_0. In the configuration space spanned by all N nuclear coordinates $(X_1, Y_1, Z_1, \cdots X_N, Y_N, Z_N)$, those configurations included in $\sum_{v_p}$ in Eq. 9 form a $3N$ dimensional region $\mathcal{D}$ around A_0.

The next step in the transition to current thermal simulations is the treatment of the ions as particles with trajectories governed by the classical equations of motion. For a system like a-Si:H, this is a defensible approximation, at least above the Debye temperature. Now, consider a MD simulation commencing from a configuration in the neighborhood of A_0. One would then approximate Eq. 9 by

$$\lim_{n\to\infty} \frac{1}{n} \sum_{j=1}^{n} \frac{2\pi}{\hbar} |\langle \Phi_{e_f}^{(j)} | F_e | \Phi_{e_i}^{(j)} \rangle|^2 \delta(\varepsilon_f^{(j)(0)} - \varepsilon_i^{(j)(0)}) d\nu_f \tag{10}$$

where n is the number of MD steps. The assumption here is that the MD trajectory faithfully reproduces the dynamical processes implicit in Eq. 2. In each MD step, the Kohn-Sham scheme gives the fully dressed single-particle energy for the electron-phonon coupling of the last MD step. In a sense, each MD step can be interpreted as a sum of one specific series of Feynman graphs in set $\mathcal{D}$, if we classify Feynman graphs according to the configuration space points in $\mathcal{D}$.

For a chosen basis set, one can expand many-electron wave function Φ as a linear combination of Slater determinants of single particle functions ψ_r,

$$\Phi_{e_q} = \sum_{q_1 q_2 \cdots q_N} e_{q_1 q_2 \cdots q_N} c_{q_1}^\dagger c_{q_2}^\dagger \cdots c_{q_N}^\dagger |000\cdots 0\rangle. \tag{11}$$

The interaction between electrons and external field $\mathbf{E}$ along the x direction can be written in single particle form as:

$$F_e = (\frac{eE}{2}) \sum_{rs} \langle \psi_r | x | \psi_s \rangle c_r^\dagger c_s \tag{12}$$

from which the usual Kubo-Greenwood formula is obtained as we discuss in the next subsection.

Depending upon the order of perturbation of Eq. 7, Eq. 9 describes various many-phonon assisted processes. This agrees with the Green function formulation. Green function method[25,26] starts from free single electron propagator and free single phonon propagator, this is contrast with Kubo formula which start with exact many-body wave function for the whole electron+phonon system. Technically, the former will be much easier than the later. Both acoustic and optical phonon assisted hopping[26] are worked out and applied to the transition rate from one localized state to another localized state, and the Meyer-Neldel relation is viewed as a consequence of assisted activation whenever large activation energies compared to typical excitation are involved[3,27].

C. Application of KGF to disordered solids at finite temperature

The derivation of the KG formula from linear response theory and the fluctuation-dissipation theorem is available in the original literature[6,7], and elementary derivations are provided in standard books on transport in amorphous systems[4,28]. In these latter derivations, first-order time-dependent perturbation theory (Fermi's Golden Rule) is employed to deduce an expression for the AC conductivity $\sigma(\omega)$. From either derivation, one expects the KGF to be valid in the weak-field limit and for elastic scattering processes. The form for the diagonal elements of the conductivity tensor for the static lattice that emerges from the preceding discussion is:

$$\begin{aligned} \sigma_{\alpha\alpha}(\omega) &= \frac{2\pi e^2 \hbar}{\Omega m^2} \sum_{ni} |\langle \psi_n | p_\alpha | \psi_i \rangle|^2 \frac{f_F(\varepsilon_i) - f_F(\varepsilon_n)}{\hbar\omega} \\ &\times \delta(\varepsilon_n - \varepsilon_i - \hbar\omega) \end{aligned} \tag{13}$$

where $\alpha = x, y, z$, f_F is the Fermi distribution, e and m are the electronic charge and mass, p_α is a component of the momentum operator, ψ_i and ε_i are the eigenstates and eigenvalues; Ω the cell volume. The AC conductivity is then $\sigma(\omega) = \frac{1}{3}\sum_\alpha \sigma_{\alpha\alpha}$. In the rest of this paper, single-particle Kohn-Sham states and eigenvalues are used for the $\{\psi\}, \{\varepsilon\}$.

In the DC-limit ($\omega \to 0$) the conductivity takes the form

$$\sigma(T) = -\frac{1}{3} \sum_\alpha \int_{-\infty}^{\infty} \sigma_{\alpha\alpha}(\varepsilon) \frac{\partial f_F(\varepsilon)}{\partial \varepsilon} d\varepsilon \tag{14}$$

where:

$$\sigma_{\alpha\alpha}(\varepsilon) = \frac{2\pi e^2 \hbar}{\Omega m^2} \sum_{ni} |\langle \psi_n | p_\alpha | \psi_i \rangle|^2 \delta(\varepsilon_n - \varepsilon) \delta(\varepsilon_i - \varepsilon), \tag{15}$$

We include thermally-induced electron state and energy fluctuations near the gap, by averaging expressions such as the preceding over a thermal simulation. The DC conductivity is computed from trajectory averaged quantities such as:

$$\overline{\sigma}_{\alpha\alpha}(\varepsilon) = \frac{2\pi e^2 \hbar}{\Omega m^2} \sum_{ni} \overline{|\langle \psi_n^t | p_\alpha | \psi_i^t \rangle|^2 \delta(\varepsilon_n^t - \varepsilon) \delta(\varepsilon_i^t - \varepsilon)}, \tag{16}$$

where the bar denotes the average and we emphasize the dependence of the various terms on the simulation time t. This average then picks up thermal broadening effects in the density of states, and also include time-dependence in the dipole matrix element. A Gaussian approximant for the δ function with a width of 0.05 eV is used in our calculations. We have repeated our calculations for widths between [0.01-0.1] eV, and our results do not change appreciably. We insert thermally averaged diagonal elements as in Eqn. 16 into Eqn 14 to obtain the conductivities reported in this paper.

The KGF includes three possible transitions: (i) localized state to localized state; (ii) localized state to extended state; (iii) extended state to extended state. For amorphous semiconductors, the upper tail of valence band and the lower tail of conduction band are localized. Below room temperature, carriers are mainly distributed in localized states, and (i) is dominant conduction mechanism. With increasing temperature, there are more holes in the upper valence tail, which are available for the electrons in lower side of mobility edge to transit. In addition, the activation energy is lowered by thermal fluctuations. At higher temperature, (ii) becomes more important until there are enough carriers in extended states, and (iii) will becomes the most effective conduction channel.

It is believed[29] that the temperature range from *ca* 300K-700K is dominated by "phonon-induced delocalization"[30], in which the phonons aid the hopping (though not to the extent of polaron formation). Phonon-induced delocalization has been computed from the time-dependent Kohn-Sham equation[14]. It was observed that if electron energies became close (because of phonon-induced variation in energies), mixing between the nearly degenerate states could occur, which results in delocalization[15]. This leads to a monotonic and irreversible decrease in electron localization. In the present calculation, the localization fluctuates (see Fig. 2 of Ref. 15). Thus, our calculation ignores the explicit phonon-driven delocalization except in so far as this effect is captured in the thermal averaging scheme.

There are sources of error in any calculation of this type, which we must mention: (1) We use the Kohn-Sham states computed in the LDA as input into the KGF. (2) We employ very small structural models (*ca* 70 atoms); (3) Except for a few test cases, we have used a minimal (single-zeta) basis. In fact we do this in part because this approximation gives a gap close to the physical gap in *a-Si*; (4) Our simulations run for finite time, though we have taken some care to verify that the reported conductivities are adequately converged; (5) There are physical mechanisms that should broaden the density of states. Two of these arise from Brillouin zone integration and the sparse and discrete sampling of the tail states due to the small cell size. (6) Classical dynamics (no quantization of the vibrations) is employed throughout. These errors are largely systematic, and as such, difficult to measure.

On the other hand, there are conditions that ameliorate the situation. Where point (1) is concerned: quasiparticle calculations for crystalline Si computed in the GW approximation and the Kohn-Sham states are nearly identical[31]. Also, there is a strong thermal averaging effect: even at room temperature, localized tail states can fluctuate by tenths of an eV (far greater than kT); this helps significantly in connection with points (2), (3) and (5) above. Finally, there is a convincing body of empirical evidence that the KGF employed as we do here (or with more primitive Hamiltonians) provides reasonably quantitative predictions for the DC conductivity. The use of a SZ basis is convenient computationally, and has the helpful feature that the gap is much closer to experiment than a complete basis calculation.

III. HAMILTONIAN AND STRUCTURAL MODELS

The *ab initio* local orbital code SIESTA[32] was used to perform the density functional calculations. We used a local density approximation for the exchange (LDA) using the Perdew and Zunger expression[33]. Norm conserving Troullier-Martins pseudopotentials[34] factorized in the Kleinman-Bylander form[35] were used. We used a minimal single ζ basis set for both Si and H[36].We solved the self consistent Kohn-Sham equations by direct diagonalization of the Hamiltonian and a conventional mixing scheme. We used the $\Gamma(k=0)$ point to sample the Brillouin zone in all calculations. No scissors correction was used since the SZ optical gap is close to experiment (a scissors shift is necessary for a polarized basis).

We have used two different well relaxed models of aSi_{64} (64 Si atoms)[37] and $aSi_{61}H_{10}$ (61 Si and 10 H atoms)[38] models. We have prepared these models for six different temperatures 200K, 300K, 500K, 700K, 1000K, and 1500K. In each cases we followed the following procedures. The two models were annealed to a particular temperature for 1.5 ps which is followed by equilibration for another 1.5 ps. Once the models are well equilibrated, we performed a constant temperature MD simulation for another 500 steps to obtain an average DC conductivity for the respected models at a given temperature.

IV. RESULTS

A. Amorphous silicon: *a-Si*

1. *Conductivity*

We have studied the electrical properties at different temperature by using the inverse participation ratio (I) which is defined as

$$\mathbf{I} = \sum_{i=1}^{N} [q_i(\varepsilon)]^2 \tag{17}$$

where N is the total number of atoms and $q_i(\varepsilon)$ is the Mulliken charge residing at an atomic site i for an eigenstate with eigenvalue ε with $\sum_{i=1}^{N}[q_i(\varepsilon)] = 1$. I is unity for an ideally localized state and $1/N$ for an extended state.

In Fig. 1 we show the instantaneous IPR as a function of energy for six different temperatures. As the temperature increases from 200K to 1500K, the optical gap is reduced and eventually at higher temperature all the

states become extended with no energy gap in the density of states. The gap closes both because of thermal fluctuations on the eigenvalues and as a harbinger of the transition to a metallic state at sufficiently high temperatures. We emphasize that these are only snapshots: the instantaneous IPR of a well-localized state can vary[15] by a factor of ≈ 2. This is understood as a consequence of the fluctuation of the eigenvalues (as eigenvalues ap-

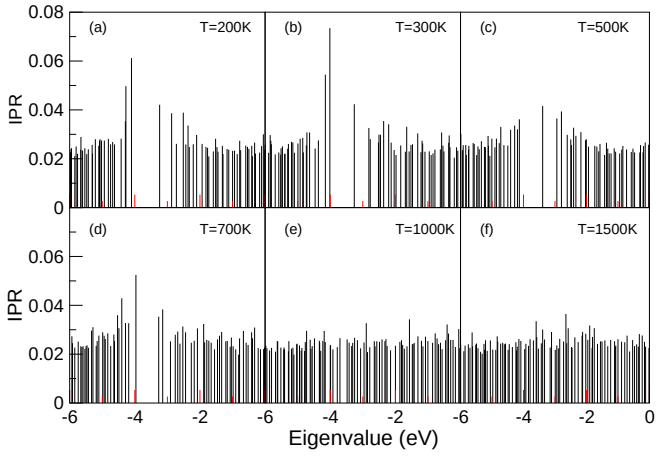

FIG. 1: Instantaneous snapshot of IPR (**I**) versus energy for different temperatures in aSi_{64} model. The Fermi level falls in the gap near $E = -3.8eV$. Localization is significant near the band edges, and note that the gap closes at higher temperature: at 1500K the cell has melted, at 1000K the gap has closed because of thermal fluctuations in the eigenvalues.

The DC conductivity of aSi_{64} is accumulated over 500 instantaneous configurations for different temperatures: T=200K, 300K , 500K, 700K, 1000K, 1500K, and 1800K. At a temperature of 1800K, the system is actually a liquid with a diffusion coefficient of $D \sim 1.6 \times 10^{-4}$ cm^{2}s^{-1} and a DC conductivity of $\sim 0.3 \times 10^4\ \Omega^{-1}$cm^{-1} which is reasonably close to the measured value of $(1.0 - 1.3) \times 10^4\ \Omega^{-1}$cm^{-1}[39] and value of $1.75 \times 10^4\ \Omega^{-1}$cm^{-1} obtained in another computation.[40].

In Fig. 2 we have shown the DC conductivity of aSi_{64} as a function of temperature. The results from experiment for selected temperatures are also shown. As we can see from Fig. 1, increase in the temperature of the system enhances delocalization of the states and eventually closes the optical gap to change the material from semiconductor to metal. In doing so the DC conductivity changes from $0.31 \times 10^{-10}\ \Omega^{-1}$cm^{-1} for T=200K to $0.24 \times 10^3\ \Omega^{-1}$cm^{-1} for T= 1000K.

The temperature dependence of DC conductivity can be written as

$$\sigma = \sigma_o e^{(-E_a/k_B T)} \tag{18}$$

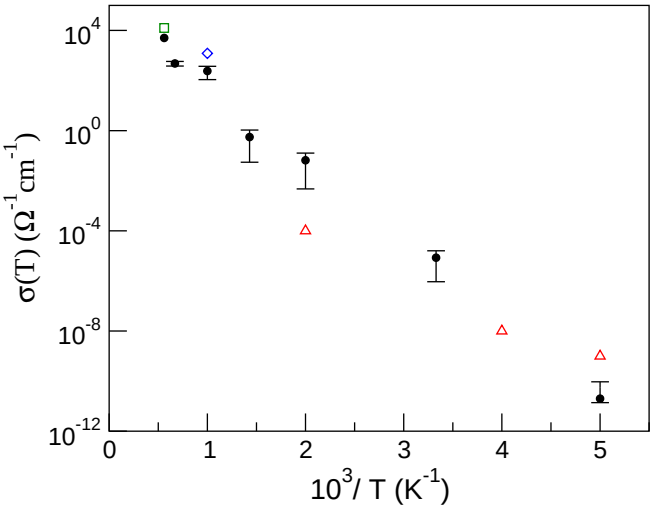

FIG. 2: (color online) DC conductivity of intrinsic aSi_{64} averaged over 500 configurations computed at different temperatures. The solid symbols are from our work, open symbols are from experiment: open square from Ref. 39, open diamond from Ref. 18 , and open triangle from Ref. 41. The error bars are from equilibration time and discrete sampling of the density of states.

where E_a is the activation energy ($E_a = E_C - E_F$ or $E_a = E_F - E_V$) and σ_o is the pre-exponential factor of the conductivity. By dividing the dc conductivity in two regions of low temperature ($T < 450K$) and high temperature ($T > 450K$) we extracted the E_a and σ_o. For low T, we have obtained $E_a \sim 0.34$ eV and $\sigma_o \sim 4\ \Omega^{-1}$cm^{-1}. For high T, $E_a \sim 0.45$ eV and $\sigma_o \sim 1 \times 10^4\ \Omega^{-1}$cm^{-1}.

B. Doping

It is known that doping and temperature change result in a shift in the position of Fermi level within the optical gap[42,43]. In our simulation, we have computed the DC conductivity for a given doping by shifting the Fermi level from its intrinsic position towards the conduction band edge or valence band edge in steps of 0.1eV. This procedure allows us to "scan" the optical gap and compute conductivity for different doping levels of n-type as well as p-type. Our scheme is quite different from experiment. For example, it is known that the energy of defect states depends upon the location of the Fermi level[44], so that a proper calculation of doping (meaning with explicit substitution of the donor or acceptor species) should be carried out self-consistently. Our procedure is a highly idealized version of the "doping problem", which shows how the conductivity varies for without compensation effects. Because of these effects, it is not easy to correlate the conductivities we predict for a specific Fermi level position with the experimental concentration of dopant

atoms. We are presently extending this work by explicitly including B and P impurities in the system and computing the conductivities separately for each doped model system.[45]

The computed DC conductivity for different temperatures as a function of chemical potential is shown in

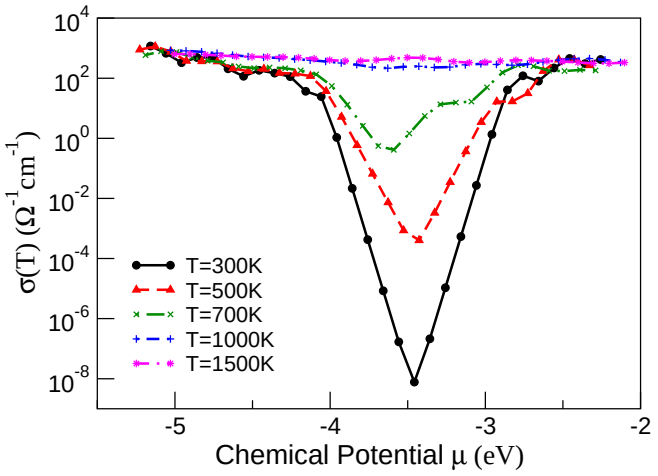

FIG. 3: (color online) DC conductivity of aSi_{64} as a function of doping, averaged over 500 configurations computed at different temperatures versus chemical potential.

C. Hydrogenated amorphous silicon: *a-Si:H*

1. *Conductivity*

In the same way we that analyzed aSi_{64} in the previous section, we have started our analysis of $aSi_{61}H_{10}$ by computing its electronic properties from the inverse participation ratio. In Fig. 4, we have shown the IPR **I** of $aSi_{61}H_{10}$ for different temperatures. As can be seen from the figure, the optical gap decreases with increasing the temperature which is attributed to phonon induced delocalization and structural rearrangements.

The DC conductivity of $aSi_{61}H_{10}$ as a function of temperature is shown in Fig. 5 with comparison from experimental results from Beyer *et al.*[46]. As we can see from Fig. 4, increase in the temperature of the system enhances delocalization of the states and eventually eliminating the optical gap to change the property of the material from semi-conductor to metal. In this case, the DC conductivity changes from 0.54×10^{-10} Ω^{-1}cm^{-1} for T=200K to 0.83×10^{2} Ω^{-1}cm^{-1} for T= 1000K.

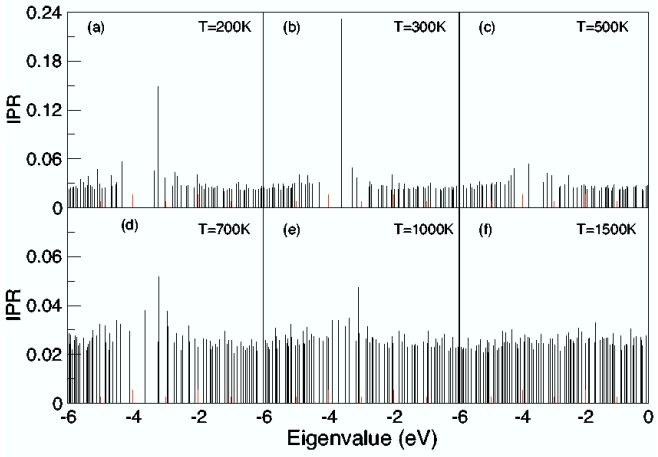

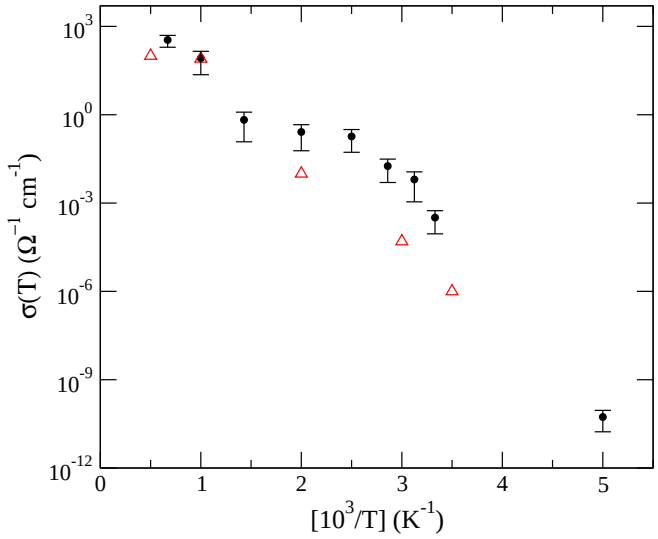

FIG. 5: (color online) DC conductivity of $aSi_{61}H_{10}$ averaged over 500 configurations computed at different temperatures. The solid symbols are from our work, open symbols are from experiment Ref. 46. The error bars are from equilibration time and discrete sampling of the density of states.

For low T, we have obtained $E_a \sim 0.31$ eV and $\sigma_o \sim 5$ Ω^{-1}cm^{-1}. For high T, $E_a \sim 0.36$ eV and $\sigma_o \sim 5 \times 10^3$ Ω^{-1}cm^{-1}. These results are in a reasonable agreement with the experimental results of Kakalios *et al.*[47]. In studying doped *a-Si:H*, Kakalios *et al.* showed that for low T, the E_a ranges from 0.16 to 0.21 eV with $\sigma_o \sim (5-10)$ Ω^{-1}cm^{-1}.

The computed DC conductivity for different temperatures as a function of chemical potential is shown in Fig. 6. As in the case of aSi_{64}, the DC conductivity increases as the Fermi energy shifts toward either the valence or conduction band from mid gap. At higher

temperature, since the optical gap is almost zero, shift-

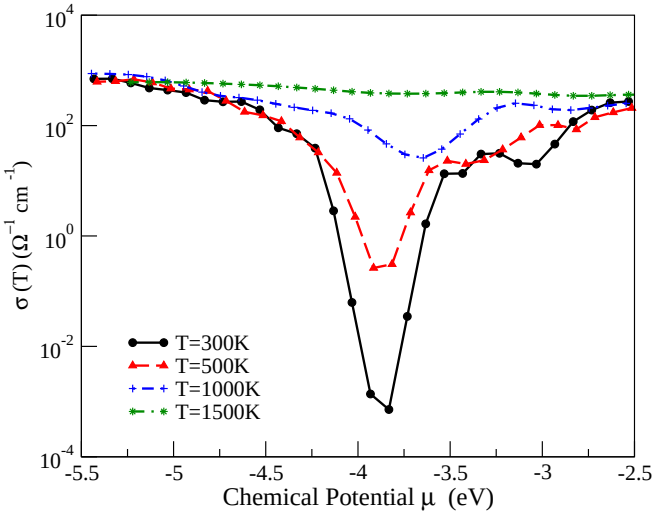

FIG. 6: (color online) DC conductivity of $aSi_{61}H_{10}$ as a function of doping, averaged over 500 configurations computed at different temperatures versus chemical potential.

As the temperature increases from 300K to 1000K, the contribution from the matrix elements decreases while the contribution from the density of states near the Fermi level increases. The temperature dependence of the DC-conductivity is most affected by the density of states which is considerably broadened for higher temperature.

2. *Meyer-Neldel rule*

In a band picture of conduction, one expects an exponential conductivity $\sigma = \sigma_0 exp(-E_a/kT)$. In disordered systems (not limited to a-Si:H) there is a more complicated T-dependence, and in particular a "kink" in the conductivity in the vicinity of 400-500K[48]. The first interpretation for this kink was the existence of distinct low-T and high-T conduction mechanisms with significantly different activation energies (slopes)[49]. It is argued that this interpretation is unlikely, and that the effect arises from the temperature dependence of the Fermi energy[48].

For activated processes with activation energy greatly exceeding the characteristic excitation energies available to the system, it is clear that a fluctuation involving many small excitations will be needed to push the system over the barrier. The larger the number of ways the necessary fluctuation may be obtained the more likely it is for the process to occur. This line of thinking led to the concept of "Multiple Excitation Entropy" (MEE), which has clarified the origin of the Meyer-Neldel Rule (MNR) in a great many different activated processes[3]. One can think of the KGF as representing a sum over pathways, in which case the number of available paths or "channels" is T-dependent and certainly increasing, reflecting an entropic increase as discussed in MEE[50].

For pre-exponential factor σ_0 and activation energy E_a, the MNR may be expressed as:

$$\sigma_o = \sigma_{oo} e^{E_a/E_{\rm MNR}} \tag{19}$$

By performing a linear fit on the DC conductivity results, we identified the intercept at $(1/T) = 0$ to σ_o and the slope to the activation energy E_a. There are number of experimental results on *a-Si:H* which show this exponential behavior with $E_{\rm MNR}$=0.067 eV[51,52]. By plotting σ as a function of $1/T$ for various dopants (n-type as well as p-type) we extracted σ_o and E_a for $aSi_{61}H_{10}$ and the results are shown in Fig. 7. Our calculation gives an exponential behavior of σ_o as a function of E_a, reflecting the Meyer-Neldel rule, with $E_{\rm MNR}$= 0.060 eV.

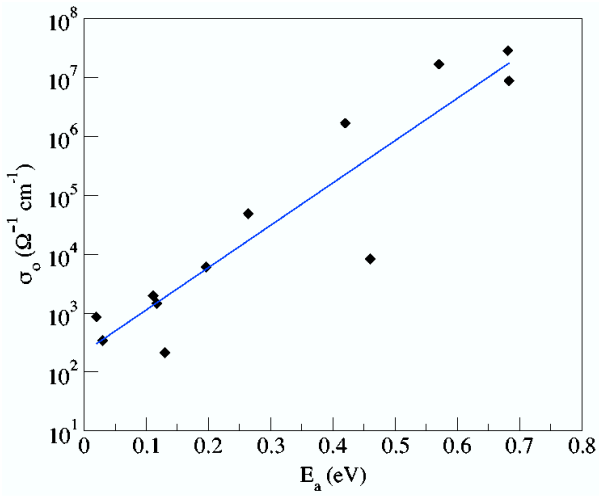

FIG. 7: (color online) The pre-exponential factor as a function of activation energy (Meyer-Neldel rule) for $aSi_{61}H_{10}$. The dashed line is an exponential fit which represent Eq. (19). It is interesting to compare this result of simulation to a similar plot for a large number of experimental samples as in Fig. 7.3 (Reference 29).

The preceding shows that the mechanism(s) responsible for MNR are present in our simulations. The enhancement of the conductivity with increased activation energy may be qualitatively understood in our picture as being due to the increase in electron-lattice coupling with increasing activation energy (and therefore localization). Since localized states possess an "amplified" electron-phonon coupling[10,11], some compensation is to be expected. In our picture, the MNR arises because the phonons treat electrons with different localization (or E_a) differently, and the effect runs in a direction consistent with experiment: for doping into the more localized states, the electron-phonon coupling is larger and serves to modulate the energies more strongly than for more weakly localized states with smaller E_a.

3. Temperature Coefficient of Resistance

The other fundamental characteristic of aSi:H is its high temperature coefficient of resistance, which makes it a candidate for uncooled microbolometer applications. The temperature coefficient of resistance (TCR) is defined as

$$TCR = \frac{1}{\rho_o}\frac{\rho - \rho_o}{T - T_o} \tag{20}$$

where ρ is a resistivity at any given temperature T and ρ_o is a resistivity at a reference temperature T_o (usually room temperature). The computed result of TCR with a definition of Eq. 20 using $T_o = 300K$ for $aSi_{61}H_{10}$ is shown in Fig. 8. The experimental TCR near room temperature is $-2.7\%K^{-1}$ for *a-Si:H*[53]. Our calculations predict a TCR value of $\sim -2.0\%K^{-1}$ at $T = 350K$ which is in agreement with the experiment. Close to T_0 the value of TCR is very sensitive to temperature and has a wide range of values $-(2.0 - 5.0)\%K^{-1}$.

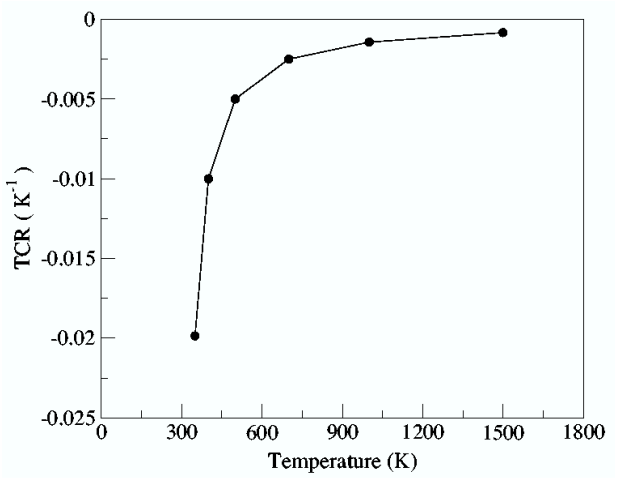

FIG. 8: The temperature coefficient of resistance (TCR) for $aSi_{61}H_{10}$ as a function of temperature.

V. CONCLUSION

We have presented a study of transport in an amorphous material. We used Kubo-Greenwood formula for computing the DC conductivity of aSi_{64} and $aSi_{61}H_{10}$ for different temperatures. We have also presented the effect of doping on the DC conductivity. As the Fermi level approaches either the conduction edge or valence edge we observe an increase in the DC conductivity. Once the E_f exceeds the "mobility edge" we observe a weak temperature dependence on the DC conductivity. Though it requires further investigation (by using various dopants in aSi_{64} and $aSi_{61}H_{10}$), we observe the Meyer-Neldel rule with exponential behavior for the pre-exponential factor σ_o. The computed result for TCR is in good agreement with the experiment. Further study of this method involves using a richer basis set, and fuller k-point sampling in the Brillouin zone (or essentially equivalently, larger cells). Further "deconstruction" of the KGF will be undertaken to explore the instantaneous configurations that provide significant contributions to σ.

Our work shows that the simplest implementation of the KGF shows promise for computing the electrical conductivity of disordered semiconductors, and this success hints that it may be used with profit on other systems beside.

VI. ACKNOWLEDGEMENTS

We thank the Army Research Office under MURI W91NF-06-2-0026, and the National Science Foundation for support under grant No. DMR 0600073, 0605890. We acknowledge helpful conversations with J. David Cohen, A. Yelon, B. Movaghar and P. Yue. Some of this work was carried out when DAD visited the Institut de Ciencia de Materials de Barcelona with support from the Programa de Movilidad de Investigadores of Minesterio de Educacion y Cultura of Spain.

* Electronic address: abtew@phy.ohiou.edu
† Electronic address: zhang@phy.ohiou.edu
‡ Electronic address: drabold@ohio.edu

[1] B. Fieque, J. L. Tissot, C. Trouilleau, A. Crastes and O. Legras Infrared Physics and Technology **49**, 187 (2007).
[2] W. Meyer and H. Neldel, Z. Techn. Phys. **12**, 588 (1937).
[3] A. Yelon, B. Movaghar and R. S. Crandall, Rep. Prog. Phys. **69** 1145 (2006).
[4] H. Overhof and P. Thomas *Electronic Transport in Hydrogenated Amorphous Silicon* Springer Tracts in Modern Physics No. 114 (Springer, Berlin, 1989) .
[5] R. M. Martin, *Electronic Structure: Basic theory and practical methods*, Cambridge University Press, Cambridge (2004).
[6] R. Kubo, J. Phys. Soc. Jpn. **12**, 570 (1957).
[7] D. A. Greenwood, Proc. Phys. Soc. **71**, 585 (1958).
[8] P. B. Allen and J. Q. Broughton, J. Phys. Chem **91** 4964 (1987).
[9] G. Zener, Proc. Phys. Soc. (London), Sect A **137**, 696 (1932).
[10] D. A. Drabold, P. A. Fedders, S. Klemm, O. F. Sankey, Phys. Rev. Lett. **67** 2179 (1991); D. A. Drabold and P. A. Fedders, Phys. Rev. B **60** R721 (1999).
[11] R. Atta-Fynn, P. Biswas and D. A. Drabold, Phys. Rev. B **69** 245204 (2004).
[12] M. Born and K. Huang, *Dynamical theory of crystal lattices*, Oxford University Press, Clarendon (1954). p. 402
[13] A. Miller and E. Abrahams, Phys. Rev. **120** 745 (1960).

[14] J. Li and D. A. Drabold, Phys. Rev. B **68** 033103 (2003).
[15] J. Li and D. A. Drabold, phys. stat. sol. (b) **233** 10 (2002).
[16] J. M. Holender and G. J. Morgan, J. Phys.: Condens. Matter **4**, 4473 (1992).
[17] J. Dong and D. A. Drabold, Phys. Rev. Lett. **80**, 1928 (1998); J. J. Ludlam, S. N. Taraskin, S. R. Elliott and D. A. Drabold, J. Phys. Cond. Matter **17** L321 (2005).
[18] S. S. Ashwin, U. V. Waghmare, and S. Sastry, Phys. Rev. Lett. **92**, 175701 (2004).
[19] J. M. Ziman, Phil. Mag. **6** 1013 (1961).
[20] M. Kaschner, M. Schone, G. Seifert and G. Pastore, J. Phys. Cond. Matt. **8** L653 (1996).
[21] P. Silvestrelli, A. Alavi and M. Parrinello, Phys. Rev. B **55** 15515 (1997).
[22] D. A. Drabold in P. Boolchand (Ed), *Insulating and Semiconducting Glasses*, World Scientific Press, Singapore (2000) p. 642.
[23] M. Brandbyge, J. L. Mozos, P. Ordejon, J. Taylor and K. Stokbro, Phys. Rev. B **65** 165401 2002.
[24] L. D. Landau and E. M. Lifshitz, Quantum Mechanics, 3rd edition, Pergamon Press, 1977.
[25] D. Emin, Phys. Rev. Lett. **32**, 303 (1974).
[26] E. Gorham-Bergeron and D. Emin, Phys. Rev. B **15**, 3667 (1977).
[27] A. Yelon and B. Movaghar, Phys. Rev. Lett. **65**, 618 (1990).
[28] N. F. Mott and E. A. Davis, *Electronic processes in non-crystalline materials* Clarendon Press (Oxford, London, 1971).
[29] R. A. Street, *Hydrogenated amorphous silicon*, Cambridge University Press, Cambridge (1991).
[30] P. Fenz, H. Muller, H. Overhof and P. Thomas, J. Phys. C **18** 3191 (1985).
[31] M. S. Hybertsen and S. G. Louie, Phys. Rev. B **34** 5390 (1986).
[32] J. M. Soler, E. Artacho, J. D. Gale, A. García, J. Junquera, P. Ordejón, and D. Sánchez-Portal, J. Phys.: Condens. Matter **14** 2745 (2002).
[33] J. P. Perdew and A. Zunger, Phys. Rev. B **23**, 5048 (1981).
[34] N. Troullier and J. L. Martins, Phys. Rev. B **43**, 1993 (1991).
[35] L. Kleinman and D. M. Bylander, Phys. Rev. Lett. **48**, 1425 (1982).
[36] This means that four (one) orbitals per site were used for Si (H).
[37] G. T. Barkema and N. Mousseau, Phys. Rev. B **62**, 4985 (2000).
[38] We removed three Si atoms from the aSi_{64} model and terminate all the dangling bonds except two with hydrogen. The newly formed supercell is then relaxed well using conjugate gradient to form a $aSi_{61}H_{10}$ model (61 Si and 10 H atoms).
[39] V. M. Glasov, S. N. Chizhevskaya, and N. N. Glagoleva, *Liquid Semiconductors* (Plenum, New York, 1969).
[40] I. Stich, R. Car, and M. Parrinello, Phys. Rev. B **44** 4262 (1991).
[41] A. Lewis, Phys. Rev. Lett. **29**, 1555 (1972).
[42] R. H. Williams, R. R. Varma, W. E. Spear, and P.G. LeComber, J. Phys. C **12**, L209 (1979).
[43] B. von Roedern, L. Ley, and M. Cardona, Solid State Commun. **29**, 415 (1979).
[44] See for example Reference 29, p. 194
[45] M. Zhang, P. Yue, T. A. Abtew and D. A. Drabold (unpublished).
[46] W. Beyer, A. Medeisis, and H. Mell, Commun. Phys. **2**, 121 (1977).
[47] J. Kakalios and R. A. Street, Phys. Rev. B **34**, 6014 (1986).
[48] H. Overhof and P. Thomas, in Ref. 22, p. 584.
[49] P. G. LeComber, A. Madam, and W. E. Spear, J. Non.-Cryst. Sol. **11** 219 (1972).
[50] B. Movaghar (private communication).
[51] D. E. Carlson and C. R. Wronski, in *Amorphous Semiconductors*, ed. by M. H. Brodski, Topics Appl. Phys., **36** (Springer, Berlin) Chap 10. (1985).
[52] H. Fritzsche, Sol. Energy Mat. **3**, 447 (1980).
[53] M. B. Dutt and V. Mittal, J. Appl. Phys. **97**, 083704 (2005).